Molecular Biology of the Cell
Vol. 21, 232–243, January 15, 2010

RSBP-1 Is a Membrane-targeting Subunit Required by the $G\alpha_q$-specific But Not the $G\alpha_o$-specific R7 Regulator of G protein Signaling in *Caenorhabditis elegans*

Morwenna Y. Porter and Michael R. Koelle

Department of Molecular Biophysics and Biochemistry, Yale University School of Medicine, New Haven, CT 06520-8024

Submitted July 31, 2009; Revised October 30, 2009; Accepted November 5, 2009
Monitoring Editor: Jonathan Chernoff

Regulator of G protein signaling (RGS) proteins inhibit G protein signaling by activating Gα GTPase activity, but the mechanisms that regulate RGS activity are not well understood. The mammalian R7 binding protein (R7BP) can interact with all members of the R7 family of RGS proteins, and palmitoylation of R7BP can target R7 RGS proteins to the plasma membrane in cultured cells. However, whether endogenous R7 RGS proteins in neurons require R7BP or membrane localization for function remains unclear. We have identified and knocked out the only apparent R7BP homolog in *Caenorhabditis elegans*, RSBP-1. Genetic studies show that loss of RSBP-1 phenocopies loss of the R7 RGS protein EAT-16, but does not disrupt function of the related R7 RGS protein EGL-10. Biochemical analyses find that EAT-16 coimmunoprecipitates with RSBP-1 and is predominantly plasma membrane-associated, whereas EGL-10 does not coimmunoprecipitate with RSBP-1 and is not predominantly membrane-associated. Mutating the conserved membrane-targeting sequence in RSBP-1 disrupts both the membrane association and function of EAT-16, demonstrating that membrane targeting by RSBP-1 is essential for EAT-16 activity. Our analysis of endogenous R7 RGS proteins in *C. elegans* neurons reveals key differences in the functional requirements for membrane targeting between members of this protein family.

INTRODUCTION

RGS (regulator of G protein signaling) proteins are key inhibitors of heterotrimeric G protein signaling. Heterotrimeric G proteins, composed of α, β, and γ subunits, transmit signals from a vast array of biological molecules to control a diverse range of cellular processes (Hamm, 1998). RGS proteins control the duration of signaling by acting as GTPase-activating proteins (GAPs) toward the α subunit of the heterotrimer, accelerating the hydrolysis of GTP and converting the G protein heterotrimer to its inactive GDP-bound state (Ross and Wilkie, 2000). Regulation of RGS protein activity provides a mechanism by which G protein signaling may be modulated in response to internal signaling events or external cues. However the mechanisms that regulate RGS activity are poorly understood.

Among the most well-studied RGS proteins are members of the R7 family. R7 RGS proteins share a conserved domain architecture and require a $G\beta_5$ subunit for stability and function. The N-terminal DEP (Dishevelled/EGL-10/Plextrin)/DHEX (DEP helical extension) domain plays a role in the subcellular targeting of the complex, the central GGL (Gγ-like) domain is required to interact with the $G\beta_5$ subunit, and the C-terminal RGS domain contains the GAP activity of the protein (Popov *et al.*, 1997; Snow *et al.*, 1998; Martemyanov *et al.*, 2003; Cheever *et al.*, 2008). Mammals have four R7 RGS proteins, RGS6, RGS7, RGS9, and RGS11, with RGS9 existing in a retinal-specific RGS9-1 isoform and an RGS9-2 isoform widely expressed in brain (Anderson *et al.*, 2009; Jayaraman *et al.*, 2009). When complexed with $G\beta_5$, all mammalian R7 RGS proteins act in vitro as GAPs with selectivity for the $G\alpha_{i/o}$ family of G proteins (Hooks *et al.*, 2003). However, whether the in vivo G protein specificity of mammalian R7 proteins matches what has been observed in vitro remains unknown.

Two recently identified membrane-targeting subunits, R9AP (RGS9 anchor protein) and R7BP (RGS7-binding protein) interact with members of the R7 RGS family (Hu and Wensel, 2002; Drenan *et al.*, 2005; Martemyanov *et al.*, 2005). In mammals R9AP is found only in the photoreceptor layer of the retina, where its C-terminal transmembrane domain anchors the RGS9-1·$G\beta_5$ complex to the disk membranes of the rod outer segments (Hu and Wensel, 2002; Keresztes *et al.*, 2003; Song *et al.*, 2007). Correct targeting of the complex to the disk membranes is required for efficient G protein inactivation (Lishko *et al.*, 2002; Hu *et al.*, 2003; Baker *et al.*, 2006). R9AP appears to be required for the stability of RGS9-1 and RGS11, because the levels of these proteins are dramatically decreased in R9AP knockout mice (Keresztes *et al.*, 2004; Cao *et al.*, 2008). R9AP knockout mice also exhibit defects in phototransduction that result from slow photoreceptor deactivation (Keresztes *et al.*, 2004). Similar phototransduction defects are seen in RGS9-1 knockout mice (Chen *et al.*, 2000) and in mice lacking the DEP domain of

This article was published online ahead of print in *MBC in Press* (http://www.molbiolcell.org/cgi/doi/10.1091/mbc.E09–07–0642) on November 18, 2009.

Address correspondence to: Michael R. Koelle (michael.koelle@yale.edu).

Abbreviations used: a.u., arbitrary units; DEP: Dishevelled/EGL-10/Plextrin; DHEX: DEP helical extension; GAP, GTPase-activating protein; GPCR, G protein–coupled receptor; PB/C, polybasic and cysteine mutant; RGS, regulator of G protein signaling; R7 RGS, R7 family regulator of G protein signaling.

RGS9-1, in which the interaction of RGS9-1 with R9AP is disrupted (Martemyanov *et al.*, 2003). Human patients with mutations in R9AP or RGS9 show defects in vision that presumably arise from analogous phototransduction defects (Nishiguchi *et al.*, 2004). Thus the RGS9-1·Gβ_5 complex requires targeting to the disk membranes by R9AP for its function as a GAP for the photoreceptor-specific Gα subunit, transducin.

In contrast to R9AP, R7BP is widely expressed throughout the nervous system, can interact with all R7 RGS protein, and does not contain a transmembrane domain to permanently anchor it to the membrane. Instead, R7BP can potentially shuttle to and from the plasma membrane by way of reversible palmitoylation (Jayaraman *et al.*, 2009). Initially regarded as a universal membrane-targeting protein for all neuronal R7 RGS proteins (Drenan *et al.*, 2005; Martemyanov *et al.*, 2005), data are now emerging that reveal differences in the requirement of various R7 RGS proteins for R7BP. Pull-down experiments from extracts of whole brain and transfected cells show that R7BP can interact with all four neuronal R7 RGS proteins (Drenan *et al.*, 2005; Martemyanov *et al.*, 2005), and both RGS7 and RGS9-2 require R7BP for membrane targeting in transfected cells that overexpress these proteins (Anderson *et al.*, 2007a,b; Grabowska *et al.*, 2008). However analysis of R7BP knockout mice found only RGS9-2 and not other R7 RGS proteins require R7BP for stability. Anderson *et al.* (2007a) showed that R7BP regulates the protein levels of RGS9-2 by protecting it from degradation by cysteine proteases. Study of the R7BP knockout mouse also showed that endogenous RGS9-2 in the brain requires R7BP for membrane targeting (Song *et al.*, 2006). However, whether the actual function of R7 RGS proteins in the brain requires membrane targeting by R7BP remains unclear. The widespread expression of R7BP in the mammalian nervous system suggests an important role in the regulation of neuronal signaling, although no strong behavioral defects have been reported for the R7BP knockout mouse. To date assays of R7 RGS function in the absence of R7BP have been limited to studies of GIRK channel kinetics in *Xenopus* oocytes heterologously expressing R7 RGS complex subunits (Drenan *et al.*, 2005, 2006). Thus questions remain regarding whether interaction with a membrane-targeting subunit is required by all R7 RGS proteins in vivo and whether membrane localization is necessary for endogenous R7 RGS complex function.

Caenorhabditis elegans contains orthologues of many mammalian G protein–coupled receptors (GPCRs), orthologues of all mammalian G protein subunits and two R7 RGS proteins, EGL-10 and EAT-16 (Bastiani and Mendel, 2006). Genetic analysis has shown that in vivo EGL-10 specifically inhibits Gα_o signaling, whereas EAT-16 specifically inhibits Gα_q signaling, presumably by exhibiting GAP activity toward these Gα subunits, although to date no in vitro GAP assays have been performed (Koelle and Horvitz, 1996; Hajdu-Cronin *et al.*, 1999). Like their mammalian counterparts, EGL-10 and EAT-16 also require a Gβ_5 subunit (Chase *et al.*, 2001; Robatzek *et al.*, 2001; van der Linden *et al.*, 2001), however before this study, no membrane-targeting subunit had been identified. We have used a combination of genetic and biochemical methods in *C. elegans* to identify a membrane-targeting subunit, RSBP-1, to investigate whether all endogenous R7 RGS·Gβ_5 complexes require a membrane-targeting subunit and to test whether membrane targeting is required for the function of R7 RGS·Gβ_5 complexes in vivo.

MATERIALS AND METHODS

Bioinformatics

RSBP-1 was identified using the BLASTP 2.0MP-WashU algorithm (http://blast.wustl.edu; Gish, 1996–2006) to search WormBase (http://www.wormbase.org, release WS168, December 27, 2006) with default parameters and a probability threshold of 1.0. Uniprot accession numbers are as follows: RSBP-1 = Q148R9; R9AP = Q9U379; and R7BP = Q8BQP9. Sequences were aligned using Lasergene MegAlign software (DNAStar, Madison, WI), α-helices were predicted using PSIPRED version 2.6 (http://bioinf.cs.ucl.ac.uk/psipred; Jones, 1999; Bryson *et al.*, 2005), and PROFsec (http://www.predictprotein.org; Rost *et al.*, 2004). Predicted α-helices in Figure 1A are regions where both programs predict α-helices in all three proteins. Minor adjustments were made to the alignment to accommodate these predictions. The transmembrane domain in mouse R9AP has previously been described (Hu and Wensel, 2002), and we predicted it using TMAP at the Biology Workbench (http://workbench.sdsc.edu; Subramaniam, 1998).

RNA Extraction

RNA was extracted from mixed-stage wild-type and *rsbp-1(vs163)* mutant animals using Trizol reagent (Invitrogen, Carlsbad, CA). Briefly, 100 μl packed worms were vortexed with four volumes Trizol, frozen in liquid nitrogen, and thawed at 37°C, and this process was repeated. Two volumes chloroform were then added, and the solution was mixed for 15 s before centrifuging at 1000 × *g* for 15 min at 4°C. The clear supernatant was transferred to a fresh tube, and RNA was precipitated in an equal volume isopropanol for 10 min at room temperature, washed in 0.5 ml 70% ethanol, resuspended in 100 μl DEPC-water, and stored at −80°C.

Reverse Transcription-PCR

First-strand cDNA was transcribed from mixed stage RNA using Moloney murine leukemia virus (M-MuLV) reverse transcriptase (Roche, Indianapolis, IN) and gene-specific primers (Integrated DNA Technologies, Coralville, IA). PCR was performed using Tgo high-fidelity polymerase (Roche). Amplicons were purified by gel extraction with QiaQuick spin columns (Qiagen, Chatsworth, CA), and sequenced by the Keck facility at Yale.

Nematode Strains and Culture

C. elegans strains were maintained under standard conditions at 20°C, and double mutants were generated using standard techniques (Brenner, 1974). *eat-16(tm761)* was obtained from the National Bioresource Project of Japan, balanced, and backcrossed to wild-type N2 six times to remove background mutations that caused lethality and sterility. For a complete list of strains used, see Supplemental Table 1.

Transgenes

Transgenic animals were generated by standard techniques (Mello and Fire, 1995). Plasmid constructs were microinjected into strains carrying the *lin-15(n765ts)* mutation in the background, using the *lin-15* rescuing plasmid, pL15EK, as a coinjection marker. For each injection, multiple transgenic lines were obtained and analyzed, as detailed below. For a complete list of transgenes and plasmids see Supplemental Tables 2 and 3, respectively.

Isolation of vs163

vs163 was isolated from a frozen library of randomly mutagenized animals, using a PCR-based strategy, as previously described (Hess *et al.*, 2006). To remove background mutations generated during the initial mutagenesis, *vs163* was backcrossed to the wild-type N2 strain four times. *vs163* is a 169-base pair deletion with the following limits: 5′-gttttacagctggtgcacga to ttttcaaaaaatctatatat-3′.

Locomotion Assays

Locomotion speed of staged adults was determined at NemaRx using a custom-built automated tracking device. Full details of this method and the technology used are provided in the Supplemental Materials.

To qualitatively analyze the depth of body bends, worms were filmed moving across a bacterial lawn using a digital video camera attached to a Leica M420 dissecting microscope (Deerfield, IL) and images of tracks in the bacterial lawn were manually traced.

Egg-laying Assays

Unlaid and early-stage egg assays were performed as previously described (Chase and Koelle, 2004). Briefly, the number of unlaid eggs was determined by dissolving adult animals in bleach and counting the bleach-resistant eggs. In Figures 3, B and E, 4A, 5A, and 7C the mean number of accumulated eggs is plotted and error bars represent 95% confidence intervals. P-values were calculated using Student's *t* test. The percentage of early-stage eggs laid was determined by allowing adult animals to lay eggs for 30 min and then visually inspecting the developmental stage of the eggs. The 95% confidence intervals

and p-values were calculated using Wilson's estimates. All assays used animals isolated as late L4 larvae and aged 30 h at 20°C to obtain precisely staged adults. In the unlaid egg assay 30 animals per genotype or 50 animals per extrachromosomal transgene (≥10 animals per independent line) were analyzed. In the early-stage egg assay, ≥100 eggs per strain or extrachromosomal transgene (≥20 eggs per independent line) were analyzed.

Generation and Fractionation of Whole Worm Lysates

C. elegans were grown in 20 ml liquid cultures at 20°C and isolated by flotation on 30% sucrose. Packed worm pellets, ~250 μl, were transferred to 2-ml straight-walled polypropylene tubes (DOT Scientific, Burton, MI) and resuspended in 1.5 ml lysis buffer (50 mM HEPES, 100 mM NaCl, 1 mM PMSF, 1 μg/ml leupeptin, 1 μg/ml pepstatin), with or without 1% Triton X-100. Lysis was by sonication on ice using a sonic dismembrator 550 (Fisher Scientific, Pittsburgh, PA) equipped with a Microtip probe, using power output set just below the microtip limit, three times for 20 s, and a program in which the 20-s process times occurred in 2-s pulses separated by 2 s to allow the sample to cool. Debris was removed by centrifugation at 800 × *g* for 10 min at 4°C. Soluble and insoluble fractions were obtained by centrifugation at 100,000 × *g* for 30 min at 4°C in a TLA120.2 rotor and Optima TLX tabletop ultracentrifuge (Beckman Coulter, Fullerton, CA). Pellet fractions were resuspended in an equal volume of lysis buffer using a dounce homogenizer. Protein concentration estimates were determined by the Bio-Rad protein assay (Richmond, CA), based on the Bradford method, using bovine serum albumin (BSA) as a standard.

Coimmunoprecipitation from Whole Worm Lysates

Soluble lysates from whole worms were generated as above and diluted in 1× PBS (137 mM NaCl, 2.7 mM KCl, 4 mM $Na_2HPO_4{\cdot}7H_2O$, 1.5 mM KH_2PO_4) to a protein concentration of 1 μg/μl. Mouse anti-FLAG-M2 antibody (3 μg, Sigma, St. Louis, MO) in 1 ml 1× PBS was bound to 50 μl protein G agarose beads (Roche) for 1 h, rotating at room temperature. Beads were washed four times in 1 ml 1× PBS for 1 min each and incubated with 500 μg whole worm lysate for 2 h, rotating at room temperature. Beads were washed four times in 1 ml 1× PBS for 1 min each and boiled in Laemmli buffer (Laemmli, 1970), minus β-mercaptoethanol, for 5 min to elute immunoprecipitated complexes. All centrifugations were at 1000 × *g* for 1 min at room temperature.

SDS-PAGE and Western Blotting

Proteins were reduced using 5% β-mercaptoethanol, fractionated on 10% SDS-PAGE gels, and transferred to nitrocellulose membranes using standard methods. Primary antibodies used were as follows: rabbit anti-EGL-10 at 1:100 (Koelle and Horvitz, 1996), rabbit anti-EAT-16 at 1:100 (generated for this study, see below), rabbit anti-GPB-2 at 1:100 (Chase *et al.*, 2001), rabbit anti-UNC-64/Syntaxin at 1:10,000 (a kind gift from M. Nonet, Washington University). The secondary antibody was HRP-conjugated goat anti-rabbit IgG at 1:3000 (Bio-Rad). To control for loading and fractionation of lysates, membranes were cut at the 45-kDa marker, the top half probed for EGL-10 or EAT-16, and the lower half was probed for the anti-UNC-64/Syntaxin control. Dashed lines on figures showing Western blots indicate where the membranes were cut. EGL-10 runs as a doublet just above 66 kDa, the EAT-16 antibody detects a single specific band just below 66 kDa and a higher cross-reactive band, GPB-2/Gβ_5 runs as a doublet at ~40 kDa, and UNC-64 runs at ~33 kDa.

EAT-16 Antibody

cDNA sequences encoding amino acids 145-473 were inserted into pET-15b to generate pMP49. 6HIS::EAT-16(145-473) was expressed in *Escherichia coli* from pMP49, purified over nickel resin in the presence of 8 M urea, and further purified by SDS-PAGE. The 6HIS::EAT-16(145-473) antigen was used by Cocalico Biologicals (Reamstown, PA) to generate polyclonal antisera in rabbits. For affinity purification of antisera, insoluble GST::EAT-16(full length), expressed from pMP53 in *E. coli*, was partially purified from inclusion bodies and immobilized on nitrocellulose membrane. After overnight incubation at 4°C with antisera, bound antibodies were eluted in 100 mM glycine, pH 2.5, and stored in 90 mM glycine, 90 mM Tris, pH 8, 5 mM sodium azide, and 1 μg/ml BSA.

Antibody Staining

Whole worms were fixed, permeabilized, and stained as described previously (Finney and Ruvkun, 1990). Primary antibodies (rabbit anti-EGL-10 and rabbit anti-EAT-16) were used at a 1:5 dilution. Secondary antibodies (Cy3-conjugated goat anti-rabbit [Invitrogen] and FITC-conjugated goat anti-rabbit [Sigma]) were used at a 1:25 dilution. To stain nuclei, after incubation in the secondary antibody, worms were washed for 25 min in PBST-B (1× PBS, 0.1% BSA, 0.5% Triton X-100, 5 mM sodium azide, 1 mM EDTA), incubated in the DNA dye ToPro3 (Invitrogen) at a 1:5000 dilution in PBST-B for 15 min, rotating at room temperature, and then were washed three times for 25 min each in PBST-B.

Confocal Microscopy

Live and fixed *C. elegans* samples were imaged on a LSM 510 confocal microscope (Zeiss, Thornwood, NY). Live animals were mounted on 4% agarose pads and anesthetized in 10 mM levamisole. Fixed animals were mounted in anti-fade solution (2.3% DABCO, 10% PBS, 90% glycerol). Fluorescence intensity across single cells was quantified using ImageJ (http://rsb.info.nih.gov/ij/; NIH). Four similar sized cells per strain or transgene were analyzed, and the mean intensity plotted to generate the graphs shown in Figure 8 and Supplemental Figure 2.

RESULTS

C. elegans *RSBP-1 Shows Similarity to Mammalian R7BP and R9AP*

Bioinformatic analysis of the complete *C. elegans* genome identified a single putative R7 RGS membrane-targeting subunit, the predicted protein T06D10.1. Mouse R9AP and mouse R7BP proteins were used in BLAST queries: T06D10.1 was the top hit in the R9AP search and the only protein retrieved using both queries. Although T06D10.1 shows only 25% identity to R9AP and 19% identity to R7BP (Figure 1, A and B), all three proteins share a conserved set of functionally significant features, described below, that we did not observe in other *C. elegans* proteins retrieved by the BLAST searches. Thus, T06D10.1 may be the only such protein in *C. elegans*, and we have named it R Seven Binding Protein-1 (RSBP-1). Expression of RSBP-1 and its gene structure were confirmed by RT-PCR. The gene is composed of five exons that encode a 171-amino acid protein (Figure 1C).

R7 RGS proteins and their membrane-targeting subunits interact via the DEP/DHEX domain of the R7 RGS proteins and three to four predicted α helices in the amino terminal portion of the membrane-targeting subunit (Baker *et al.*, 2006; Anderson *et al.*, 2007b). Analysis of the predicted secondary structure of RSBP-1 suggests that RSBP-1 contains four predicted α helices, and the greatest sequence similarity between all three proteins lies in the first three predicted α helices (Figure 1A).

Mammalian R7-binding proteins use two different C-terminal targeting sequences for plasma membrane attachment. A transmembrane domain anchors R9AP (Hu and Wensel, 2002), whereas R7BP uses a string of basic residues and two palmitoylation sites to reversibly tether to the plasma membrane (Drenan *et al.*, 2005). The RSBP-1 C-terminus is not predicted to contain a transmembrane domain, but does contain a string of four basic residues and three cysteine residues that may be palmitoylated. This suggests that RSBP-1 could tether to the plasma membrane in the same manner as R7BP (Figure 1B). RSBP-1 is the only protein that we have identified in the *C. elegans* genome that contains all known functionally important features of an R7 RGS membrane-targeting subunit.

rsbp-1 Mutants Phenocopy eat-16 Mutants

To determine whether RSBP-1 is required for the function of R7 RGS proteins in *C. elegans*, we generated a knockout allele, *vs163*, and examined its phenotype. The 169-base pair *vs163* deletion removes exon two, and RT-PCR shows that exon one splices directly to exon three, resulting in a reading frame shift. The resulting transcript encodes a truncated protein with only the first 14 amino acids of RSBP-1, encoded by exon 1, followed by 13 extraneous amino acids (Figure 1, A and C). Thus *vs163* is a null allele and we refer to it henceforth as *rsbp-1(null). rsbp-1(null)* mutants exhibited gross morphological and behavioral defects qualitatively indistinguishable from those of *eat-16(null)* mutants. Mutants for both genes are skinny, pale, develop slowly and are hyperactive for egg-laying and locomotion behaviors.

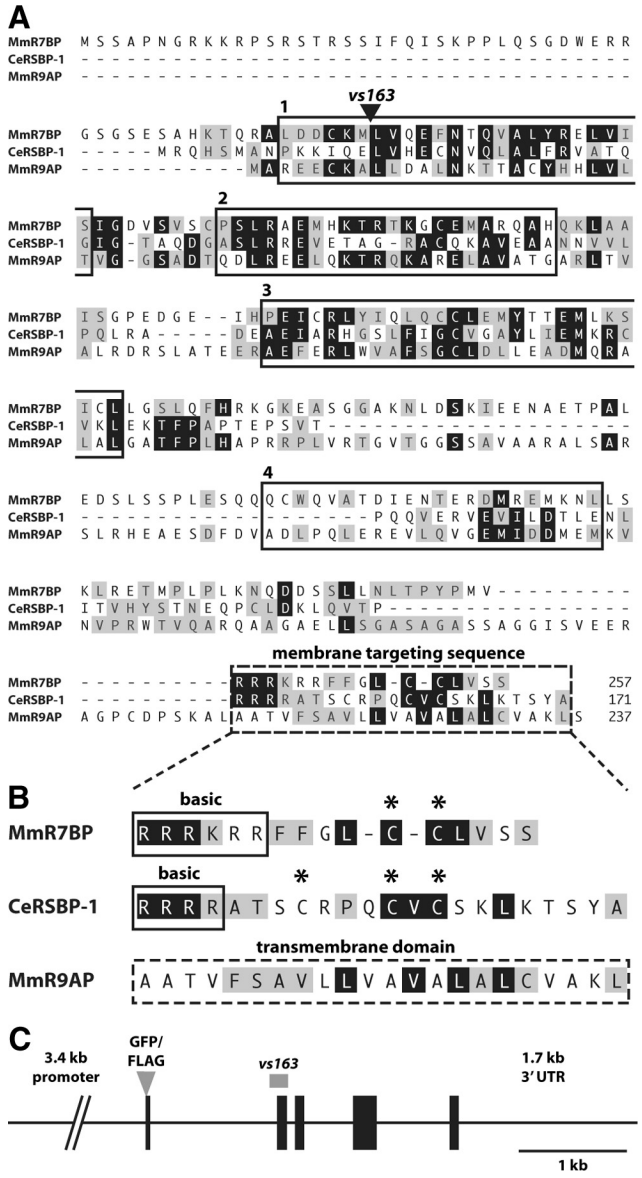

Figure 1. Identification of an R7 RGS membrane-targeting protein in *C. elegans*. (A) Alignment of mouse R7BP (MmR7BP), *C. elegans* RSBP-1 (CeRSBP-1), and mouse R9AP (MmR9AP) showing conserved sequence and structural elements. Identical amino acids (■), functionally similar amino acids (▨), predicted α helices (solid boxes numbered 1–4), and the C-terminal membrane-targeting sequences (dashed box) are indicated. An arrowhead marks the site at which CeRSBP-1 is truncated by the *vs163* deletion. (B) Expanded view of the C-terminal membrane-targeting sequence. The polybasic region of MmR7BP and CeRSBP-1 (basic, solid box), confirmed palmitoylated cysteine residues in MmR7BP (asterisks), putative palmitoylated cysteine residues in CeRSBP-1 (asterisks) and the transmembrane domain of MmR9AP (dashed box) are indicated. The targeting sequence of MmR7BP is conserved in CeRSBP-1. (C) Schematic of the *C. elegans rsbp-1* gene. Protein coding exons (■), the 169-base pair *vs163* deletion (▨), and the insertion site for GFP or FLAG tags (gray triangle) are indicated. In transgenic rescue experiments, genomic clones containing 3.4 kb of promoter region upstream of the *rsbp-1* start codon and 1.7 kb of 3′ UTR downstream of the *rsbp-1* stop codon were used.

Wild-type animals move across a bacterial lawn using sinusoidal body bends, making occasional reversals, whereas *eat-16(null)* mutants move faster and with deeper body bends (Hajdu-Cronin *et al.*, 1999). We used a video camera and automated tracking software to analyze animals as they moved across a bacterial lawn. We found that wild-type animals moved with an average speed of 6.58 ± 0.19 a.u. (Figure 2A), whereas *eat-16(null)* and *rsbp-1(null)* mutants moved faster at 9.71 ± 0.29 and 9.12 ± 0.28 a.u., respectively (Figure 2, C and E). The difference in mean speed arises from differences in the distribution of speeds within the different populations. Although the most frequently measured speeds (the modes of the distributions) were 2–3 a.u. for all three populations, the *eat-16(null)* and *rsbp-1(null)* populations moved faster on average because of greater proportions of fast-moving animals (Figure 2, A, C, and E). Additional video analysis showed that in comparison to wild-type animals (Figure 2B and Supplemental Movie 1), both *eat-16(null)* and *rsbp-1(null)* mutants moved with deeper body bends (Figure 2, D and F, and Supplemental Movies 2 and 3) and made more reversals (data not shown). Thus *rsbp-1(null)* mutants show a set of specific defects in locomotion similar to those seen in *eat-16(null)* mutants.

Wild-type animals hold their eggs in utero for a few hours after fertilization while the embryos develop past the eight-cell stage. However hyperactive *eat-16(null)* mutants lay their eggs almost as soon as they are fertilized, so that few eggs accumulate in utero and the eggs laid are at an early developmental stage of eight cells or less. We found that wild-type animals accumulated an average of 14.5 ± 0.9 eggs per adult (Figure 2I), whereas *eat-16(null)* and *rsbp-1(null)* mutants accumulated only 2.3 ± 0.4 and 2.1 ± 0.4 unlaid eggs per adult, respectively (Figure 2, J and K). In addition, wild-type animals laid only 22% of their eggs at an early developmental stage, whereas *eat-16(null)* and *rsbp-1(null)* mutants laid 90 and 92% early-stage eggs, respectively (Supplemental Figure 1A, bars 1, 3, and 6). We conclude that *rsbp-1(null)* mutants show hyperactive egg-laying behavior similar to that of *eat-16(null)* mutants.

To confirm that the hyperactive behaviors observed in *rsbp-1(null)* mutants were caused by the *vs163* deletion, we used a wild-type *rsbp-1* genomic clone as a transgene to rescue the phenotype of *rsbp-1(null)* mutants. In animals expressing this transgene, locomotion and egg-laying behaviors were restored toward wild-type levels. Transgenic animals moved at an average speed of 5.77 ± 0.17 a.u. (Figure 2G) and in a normal sinusoidal wave (Figure 2H and Supplemental Movie 4) with few reversals. In addition, *rsbp-1(null)* mutants expressing the *rsbp-1* transgene, accumulated 11.5 ± 1.4 unlaid eggs (Figure 2L) and laid only 17% early-stage eggs (Supplemental Figure 1B, bar 5). We note that both locomotion and egg-laying behavior are mildly decreased in animals expressing the transgene relative to wild-type animals, defects opposite those seen in *rsbp-1(null)* mutants. We attribute this to overexpression of the RSBP-1 protein because the transgene is expressed from a multicopy array.

RSBP-1 Is Required for the Function of EAT-16 But Not EGL-10

Our phenotypic analysis of *rsbp-1(null)* mutants suggested loss of RSBP-1 may disrupt the function of EAT-16 but not affect the function of the other *C. elegans* R7 RGS protein, EGL-10. We investigated this hypothesis by analyzing the function and protein levels of endogenous R7 RGS proteins in animals lacking RSBP-1. Our functional analysis used egg laying as a readout of G protein signaling (Figure 3 and Supplemental Figure 1). As schematized in Figure 3A, sig-

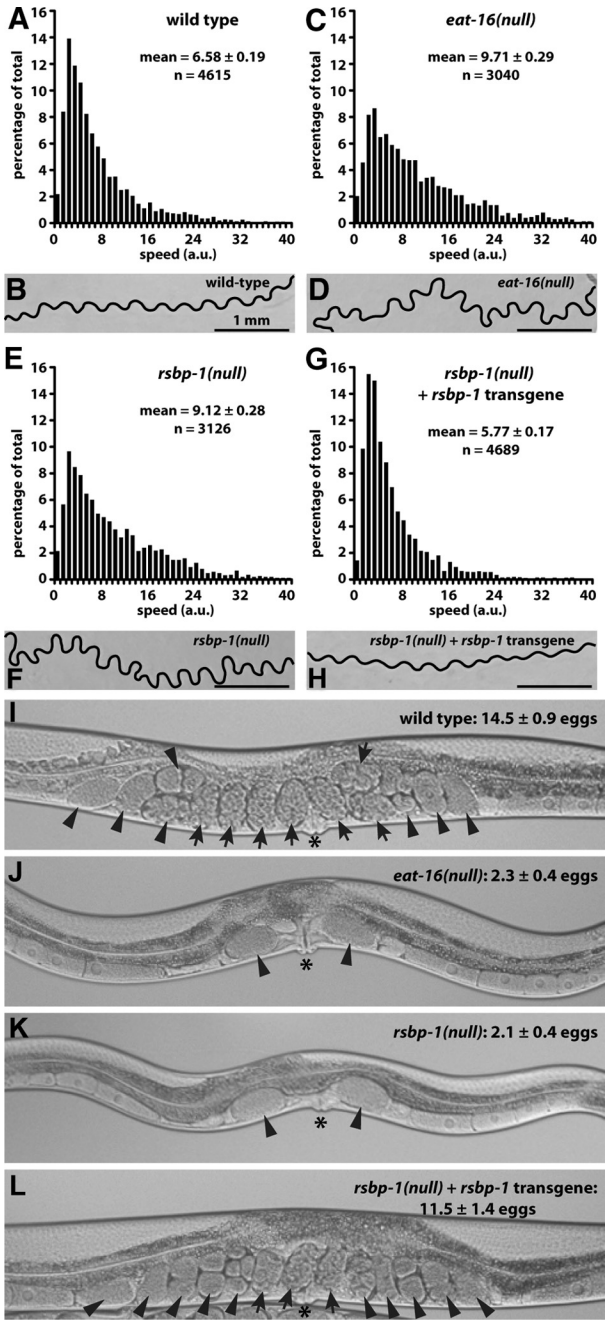

Figure 2. Locomotion and egg-laying behavior in wild-type animals, *rsbp-1* mutants, *eat-16* mutants, and *rsbp-1* mutants expressing a rescuing *rsbp-1* transgene. (A, C, E, and G) Speed distribution of the indicated genotypes. The speed of individual animals, measured in arbitrary units (a.u.), is plotted against the percentage of the population moving at each speed. Mean speed ± 95% confidence interval and the number of measurements (n) are indicated. (B, D, F, and H) Representative tracks made by animals of the indicated genotypes as they cross a bacterial lawn. Scale bars, 1 mm. Original movies of animals making tracks are available as Supplemental Movies 1–4. (I-L) Images showing unlaid eggs in representative animals of the indicated genotypes. The mean number of eggs accumulated by each strain ± 95% confidence interval, the vulva (asterisks), 1–8 cell eggs (arrowheads), and >8 cell eggs (arrows) are indicated. *eat-16(null)* and *rsbp-1(null)* mutants moved faster ($p < 0.0001$), with deeper body bends and accumulated fewer eggs ($p < 0.0001$) than did wild-type animals, and these defects were rescued beyond wild-type levels ($p < 0.0001$) in *rsbp-1(null)* mutants expressing an *rsbp-1* transgene.

naling by $G\alpha_o$ inhibits egg laying, whereas signaling by $G\alpha_q$ stimulates egg laying (Mendel *et al.*, 1995; Ségalat *et al.*, 1995; Brundage *et al.*, 1996; Schafer, 2005). The two R7 RGS proteins, EGL-10 and EAT-16, terminate $G\alpha_o$ and $G\alpha_q$ signaling, respectively, presumably via GTPase activation, thus maintaining the balance of signaling between these opposing G proteins (Porter and Koelle, 2009). The $G\beta_5$/GPB-2 subunit is required for both EGL-10 and EAT-16 function (Chase *et al.*, 2001; Robatzek *et al.*, 2001; van der Linden *et al.*, 2001).

We first observed in a series of control experiments that wild-type animals accumulated ~14 unlaid eggs in utero (Figure 3B, bar 1), whereas *egl-10* mutants (with increased inhibitory $G\alpha_o$ signaling) accumulated far more (Figure 3B, bar 2) and *eat-16* mutants (with increased stimulatory $G\alpha_q$ signaling) accumulated far less (Figure 3B, bar 3). Western blots confirmed that each mutant lacked the corresponding R7 RGS protein (Figure 3, C and D, lanes 1–3). Loss of both R7 RGS proteins, in *eat-16(null); egl-10(null)* double mutants or GPB-2/$G\beta_5$ mutants, resulted in animals whose egg laying more closely resembled that of wild-type animals than that of animals lacking only a single R7 RGS protein, apparently because comparable increases in signaling by both $G\alpha_o$ and $G\alpha_q$ restore the overall balance of signaling (Figure 3B, bars 4 and 5). Western blots confirmed the absence or reduction of both EGL-10 and EAT-16 protein in these strains (Figure 3, C and D, lanes 4 and 5). These data were consistent with previous analyses (Koelle and Horvitz, 1996; Hajdu-Cronin *et al.*, 1999; Chase *et al.*, 2001; Robatzek *et al.*, 2001; van der Linden *et al.*, 2001).

We next analyzed the effects of the *rsbp-1(null)* mutation. In support of the hypothesis that the strong hyperactive egg laying observed in *rsbp-1(null)* mutants (Figures 2K and 3B, bar 6) was caused by loss of EAT-16 but not EGL-10 function, we found by Western analysis that EAT-16 protein levels were drastically decreased in the *rsbp-1(null)* mutant, whereas EGL-10 was present at wild-type levels (Figure 3, C and D, lane 6). Further support for the hypothesis came from the observation that the *rsbp-1(null); egl-10(null)* double mutants, in which the EAT-16 protein was decreased and EGL-10 was absent, accumulated 14.9 ± 1.6 unlaid eggs (Figure 3B, bar 7), similar to that observed in the wild type and in *eat-16(null); egl-10(null)* double mutants. We were unable to generate an *eat-16 rsbp-1* double mutant for analysis because of the close genomic proximity of these two genes (0.3 map units apart on chromosome I).

Finally, we tested whether RSBP-1 is required for the effects of overexpressing EAT-16. We overexpressed EAT-16 using a transgene carrying multiple copies of an *eat-16* genomic clone. In a wild-type background, the *eat-16* overexpression transgene increased the number of unlaid eggs that accumulated (Figure 3E), presumably by inhibiting $G\alpha_q$ signaling. However, the multicopy *eat-16* transgene caused no changes in egg-laying behavior of the *rsbp-1(null)* mutant (Figure 3E). Thus the effects of overexpressing EAT-16 require RSBP-1.

Our analysis indicates that the hyperactive egg-laying and other behavioral defects seen in *rsbp-1(null)* mutants are the result of decreased EAT-16 protein levels and function, and thus increased $G\alpha_q$ signaling. Our data suggest that RSBP-1, like GPB-2/$G\beta_5$, is an essential subunit of the EAT-16 complex required for both the stability and function of the EAT-16 protein. In contrast, we saw no evidence that RSBP-1 affects EGL-10 protein levels or function.

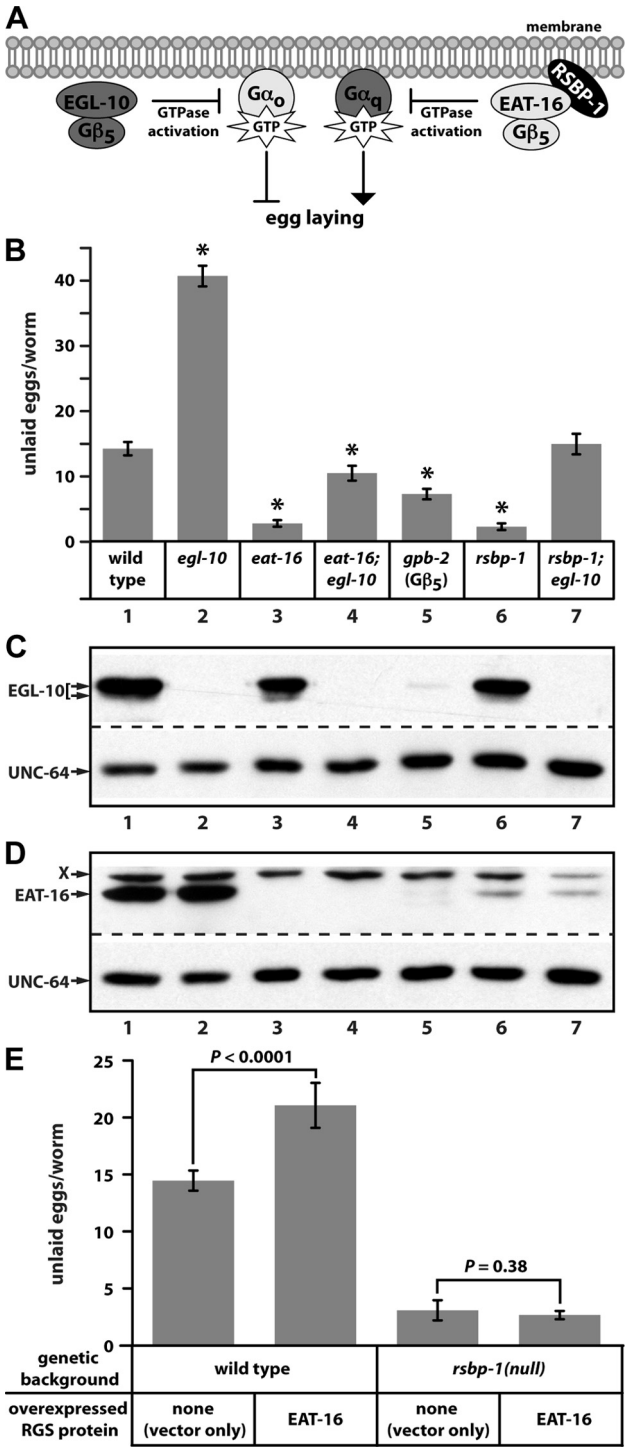

Figure 3. Egg-laying behavior and R7 RGS protein levels in mutants lacking combinations of R7 RGS protein subunits. (A) Schematic of R7 RGS regulation of G protein signaling in *C. elegans*. Our data suggests RSBP-1 is required for the function of only EAT-16. (B) Egg-laying behavior in the indicated genotypes. In this and subsequent figures, the mean number of accumulated unlaid eggs is plotted, error bars represent 95% confidence intervals, and asterisks indicate values different from the wild-type control, with $p < 0.0001$. (C and D) Western blot analysis of EGL-10 and EAT-16 protein levels in lysates of whole animals of the indicated genotypes. EGL-10 runs as a doublet, the EAT-16 antibody detects a single specific band and a higher cross-reactive band (X), UNC-64/syntaxin is the loading control. Lanes 1–7 correspond to the same genotypes analyzed in B. The level of EAT-16 but not EGL-10 protein is decreased in animals containing the *rsbp-1(null)* mutation. (E) Egg-laying behavior in wild-type or *rsbp-1(null)* mutants carrying vector alone or *eat-16* overexpressing transgenes. Overexpression of EAT-16 in wild-type animals increased the number of accumulated unlaid eggs, whereas overexpression of EAT-16 in *rsbp-1(null)* mutants had no effect compared with the control.

Endogenous EAT-16 But Not EGL-10 Coimmunoprecipitates with RSBP-1

To determine whether RSBP-1 is a subunit of either or both R7 RGS complexes in *C. elegans*, we generated a functional epitope-tagged version of the protein (FLAG::RSBP-1) and used it in coimmunoprecipitation experiments with anti-FLAG antibodies. A transgene expressing FLAG::RSBP-1, but not a vector-only control, restored egg laying in *rsbp-1(null)* mutants to wild-type levels and confirmed that the tagged protein was functional (Figure 4A and Supplemental Figure 1B). We found that FLAG::RSBP-1, but not untagged RSBP-1 used as a negative control (Figure 4B, lane 1 and 2), caused coimmunoprecipitation of EAT-16 and GPB-2/Gβ_5 but not EGL-10 from lysates of whole animals (Figure 4B, lanes 3 and 4).

RSBP-1 might interact strongly with EAT-16 and only weakly with EGL-10, such that EAT-16 outcompetes EGL-10 for association with a limited pool of RSBP-1 protein. To test this possibility, we expressed FLAG::RSBP-1 in *eat-16(null)* mutants, immunoprecipitated with anti-FLAG antibodies. We still did not pull down EGL-10, EAT-16, or GPB-2/Gβ_5 from these animals (Figure 4B, lanes 5 and 6). We also expressed FLAG::RSBP-1 in *egl-10(null)* mutants and could still pull down EAT-16 and GPB-2/Gβ_5 from these animals (Figure 4B, lanes 7 and 8). Our results indicate that RSBP-1 interacts with the EAT-16·GPB-2/Gβ_5 complex but not the EGL-10·GPB-2/Gβ_5 complex. Although it remains possible that RSBP-1 could have a very low affinity interaction with EGL-10·GPB-2/Gβ_5, this was not detected in our experiments. The combined data from our genetic experiments and immunoprecipitations strongly support a model in which RSBP-1 does not interact with endogenous EGL-10 protein and is not required for its function.

RSBP-1 Is Expressed throughout the C. elegans *Nervous System and in Muscles*

To determine where *RSBP-1* is expressed in *C. elegans*, we generated a functional green fluorescent protein (GFP)-tagged version of RSBP-1 (GFP::RSBP-1) and analyzed its expression pattern. The GFP::RSBP-1 transgene, but not a vector-only control, restored egg laying to wild-type levels in *rsbp-1(null)* mutants, confirming that the tagged protein was functional (Figure 5A and Supplemental Figure 1B). We found that GFP::RSBP-1 was expressed throughout the *C. elegans* nervous system and in many muscles (Figure 5B). This expression pattern is similar to those previously reported for EGL-10, EAT-16, GPB-2/Gβ_5, Gα_o, and Gα_q (Koelle and Horvitz, 1996; Hajdu-Cronin *et al.*, 1999; Chase *et al.*, 2001; van der Linden *et al.*, 2001; Bastiani and Mendel, 2006) We observed expression of GFP::RSBP-1 in neuronal cell bodies in the head, in the bundle of neuronal processes that form the nerve ring and in the neurons and muscles of the pharynx (Figure 5C); in neuronal cell bodies and the anal depressor muscle in the tail (Figure 5D); in the cell bodies and processes of the ventral nerve cord and in body wall muscles, which are required for locomotion (Figure 5E); in the hermaphrodite specific neuron (HSN) and the vulval

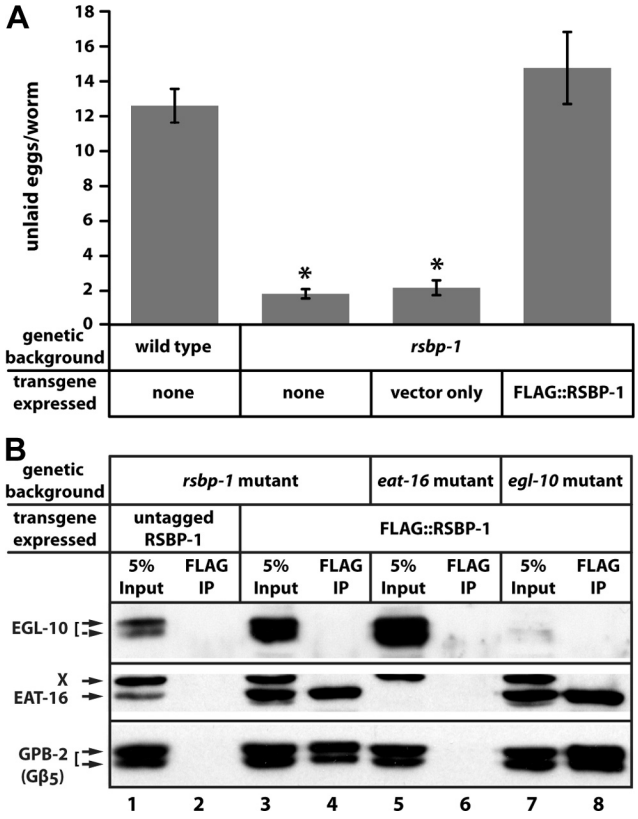

Figure 4. Coimmunoprecipitation of R7 RGS complexes by functional FLAG-tagged RSBP-1. (A) Egg-laying behavior of wild-type animals or *rsbp-1(null)* mutants carrying the indicated transgenes. Expression of FLAG::RSBP-1 in *rsbp-1(null)* mutants restored egg laying to wild-type levels. Asterisks indicate values different from the wild-type control with $p < 0.0001$. (B) Anti-FLAG coimmunoprecipitation of R7 RGS complexes from lysates of animals of the indicated genotypes. Untagged RSBP-1 expressed in *rsbp-1(null)* mutants served as a negative control. Samples representing 5% of the input material (5% input) and the whole immunoprecipitated pellet (FLAG IP) were analyzed by Western blotting. EGL-10 runs as a doublet, anti-EAT-16 detects a single specific band and a higher cross-reactive band (X), and GPB-2/Gβ_5 runs as a doublet. Expression of untagged RSBP-1 did not result in immunoprecipitation of any R7 RGS complexes (lanes 1 and 2). Using lysates of animals expressing FLAG::RSBP-1, EAT-16, and GPB-2/Gβ_5 but not EGL-10 coimmunoprecipitated (lanes 3 and 4). In *eat-16(null)* mutants, all GPB-2/Gβ_5 is in complex with EGL-10, and neither EGL-10 nor GPB-2/Gβ_5 coimmunoprecipitated (lanes 5 and 6). In *egl-10(null)* mutants, all GPB-2/Gβ_5 is in complex with EAT-16, and EAT-16 and GPB-2/Gβ_5 coimmunoprecipitated (lanes 7, 8). Thus FLAG::RSBP-1 coimmunoprecipitates with the EAT-16·GPB-2/Gβ_5 complex, but not with the EGL-10·GPB-2/Gβ_5 complex.

and uterine muscles that are required for egg laying (Figure 5F); as well as in lateral neurons, the dorsal nerve cord, commissural nerve processes, and additional muscles and support cells in the head (data not shown). We note that the GFP::RSBP-1 fusion protein is overexpressed, and we therefore cannot make any conclusions with regard to the subcellular localization of this protein.

EAT-16 But Not EGL-10 Is a Predominantly Membrane-associated Protein

To determine whether RSBP-1 is required for the membrane targeting of either R7 RGS protein, we analyzed their subcellular localization in wild-type and *rsbp-1(null)* animals.

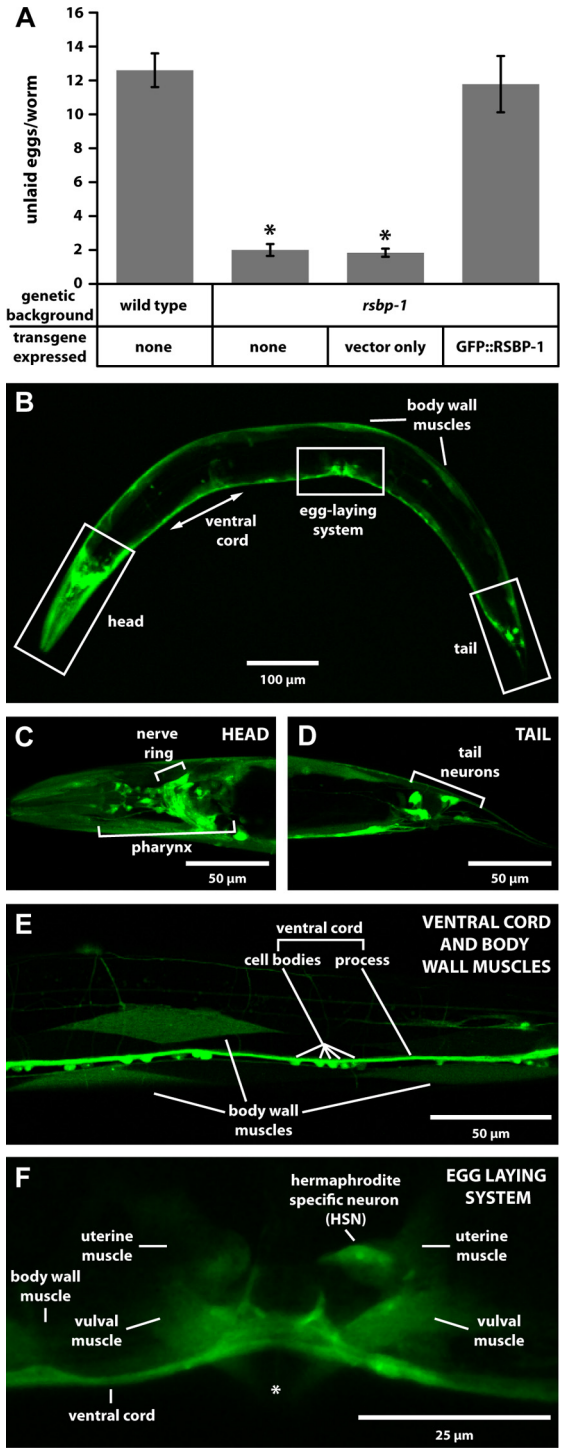

Figure 5. Expression pattern of a functional GFP::RSBP-1 transgene. (A) Egg-laying behavior of wild-type animals or *rsbp-1(null)* mutants carrying the indicated transgenes. Expression of GFP::RSBP-1 in *rsbp-1(null)* mutants restored egg laying to wild-type levels. Asterisks indicate values different from the wild-type control, with $p < 0.0001$. Localization of GFP::RSBP-1 in (B) a whole worm, (C) head, (D) tail, (E) ventral nerve cord and body wall muscles, and (F) the egg-laying system. Specific cell types and scale bars are indicated. In F an asterisk marks the vulva. GFP::RSBP-1 is expressed in neurons and muscles throughout the animal including those that control locomotion and egg-laying behaviors.

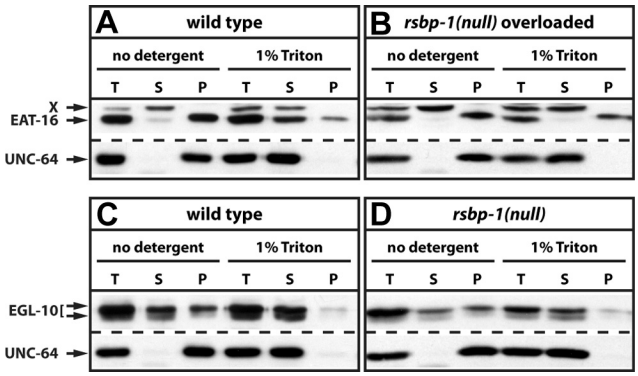

Figure 6. Subcellular fractionation of EAT-16 and EGL-10 in wild-type and *rsbp-1(null)* animals. (A–D) Whole worm lysates of the indicated genotypes were fractionated with or without detergent, and total (T), supernatant/soluble (S), and pellet/membrane (P) fractions were analyzed by Western blotting with anti-EAT-16 and anti-EGL-10 antibodies. UNC-64/Syntaxin was used as a control membrane protein to assess fractionation efficiency: in the absence of detergent, membrane-associated proteins are found in the pellet fraction and can be moved to the soluble fraction by adding 1% Triton X-100. In the absence of RSBP-1, EAT-16 levels are decreased, therefore in B the gel was loaded with three times as much protein as used in other experiments. (A) In wild-type animals EAT-16 was predominantly membrane-associated. (B) In *rsbp-1(null)* mutants the small portion of EAT-16 that remained pelleted but was not solubilized by detergent. (C) In wild-type animals, EGL-10 was predominantly soluble. (D) In *rsbp-1(null)* mutants, EGL-10 fractionation was unchanged.

Lysates of whole worms were centrifuged at 100,000 × *g*, and the distribution of each R7 RGS protein to the supernatant (soluble) and pellet (membrane) fractions was determined by Western analysis.

We found that EAT-16 is predominantly membrane-associated. The majority of EAT-16 in wild-type animals fractionated in the pellet in the absence of detergent and was solubilized by the addition of the nonionic detergent Triton X-100 (Figure 6A). Analysis of EAT-16 fractionation in *rsbp-1(null)* mutants was complicated by the reduction in EAT-16 levels; however, loading three times as much total protein on our Western blots allowed us to detect a measurable signal. In *rsbp-1(null)* mutants the residual EAT-16 protein was still found in the pellet fraction in the absence of detergent but could not be solubilized by the addition of Triton X-100 (Figure 6B). This partitioning is not typical for a membrane-associated protein and suggests the residual EAT-16 protein may be misfolded or associated with cytoskeletal structures or a detergent-resistant membrane microdomain. To further analyze the subcellular localization of EAT-16, we immunostained wild-type and *rsbp-1(null)* animals with our EAT-16 antibody. In wild-type animals EAT-16 staining was observed in tight rings around neuronal cell bodies, consistent with plasma membrane localization (Supplemental Figure 2, A and E). This staining was absent in *eat-16(null)* mutants confirming the specificity of our antibody (data not shown). We were unable to detect EAT-16 staining in *rsbp-1(null)* mutants (Supplemental Figure 2, B and E) and thus could not satisfactorily assess localization of the small amount of residual EAT-16 protein in these animals.

In contrast to EAT-16, EGL-10 was found primarily in the supernatant and thus not membrane-associated. The small fraction of EGL-10 that did pellet was mostly solubilized by addition of nonionic detergent, indicating that this portion was membrane-associated (Figure 6C). The presence of a large soluble pool of EGL-10 was somewhat unexpected, as membrane localization is thought to be required for RGS proteins to act as GTPase activators of their membrane-localized Gα targets (Hu *et al.*, 2003; Drenan *et al.*, 2005, 2006; Baker *et al.*, 2006). Consistent with our genetic and immunoprecipitation results indicating no role for RSBP-1 in EGL-10 function, the fractionation pattern of EGL-10 remained unchanged in *rsbp-1(null)* mutants (Figure 6D). Similarly, EGL-10 antibody staining revealed no differences between wild-type and *rsbp-1(null)* animals (Supplemental Figure 2, C, D, and F).

The C-Terminal Membrane-targeting Region of RSBP-1 Is Required for EAT-16 Function

To determine whether the putative C-terminal targeting sequence of RSBP-1 is required for the function and localization of EAT-16, we generated transgenic animals expressing a mutant form of FLAG::RSBP-1 that lacked the putative membrane-targeting sequence. We used this approach because the very low levels of EAT-16 in *rsbp-1(null)* mutants prevented us from satisfactorily assessing this question in these animals. We neutralized the polybasic region by mutating two of four arginines to glutamate and we mutated the three C-terminal cysteine residues to alanines to prevent palmitoylation (Figure 7A). We refer to this mutant henceforth as FLAG::RSBP-1(PB/C) (polybasic and cysteine mutant). This approach has previously been used to disrupt membrane targeting of R7BP in mammalian cell culture (Drenan *et al.*, 2005; Song *et al.*, 2006).

We found that wild-type FLAG::RSBP-1 and FLAG::RSBP-1(PB/C) both coimmunoprecipitated with EAT-16 and GPB-2/Gβ_5 (Figure 7B). Thus mutation of the C-terminal targeting sequence does not alter the interaction of RSBP-1 with the EAT-16·GPB-2/Gβ_5 complex.

Next we examined whether FLAG::RSBP-1(PB/C) was functional by analyzing egg-laying behavior and EAT-16 protein levels in *rsbp-1(null)* mutants expressing FLAG::RSBP-1(PB/C). We found that although wild-type FLAG::RSBP-1 restored egg-laying behavior to wild-type levels (Figure 7C, bars 1–4, and Supplemental Figure 1B), the mutant FLAG::RSBP-1(PB/C) protein did not rescue the egg-laying defects of *rsbp-1(null)* animals (Figure 7C, bar 5, and Supplemental Figure 1B). Thus FLAG::RSBP-1(PB/C) is not functional. Nevertheless, our Western analysis showed EAT-16 levels are restored in *rsbp-1(null)* mutants expressing either the wild-type or PB/C mutant form of FLAG::RSBP-1 (Figure 7D). We thus conclude that the putative membrane-targeting sequence in RSBP-1 is required for the function of EAT-16 but is not required for interaction with EAT-16·GPB-2/Gβ_5, nor to maintain endogenous EAT-16 protein levels.

The C Terminal Membrane-targeting Region of RSBP-1 Is Required to Target EAT-16 to the Plasma Membrane

To determine whether the putative membrane-targeting sequence of RSBP-1 is required to target EAT-16 to its presumed site of action at the plasma membrane, we analyzed the subcellular localization of EAT-16 in animals expressing wild-type or targeting-deficient FLAG::RSBP-1. In *rsbp-1(null)* animals expressing wild-type FLAG::RSBP-1, the majority of EAT-16 was found in the pellet (membrane) fraction in the absence of detergent and was solubilized by the addition of Triton X-100 (Figure 8A). This was the same as we had observed previously in wild-type animals, in which endogenous RSBP-1 targets EAT-16 to the membrane fraction (Figure 6A). In contrast, EAT-16 was predominantly found in the soluble (cytoplasmic) fraction in *rsbp-1(null)* animals expressing FLAG::RSBP-1(PB/C) (Figure 8B). Thus

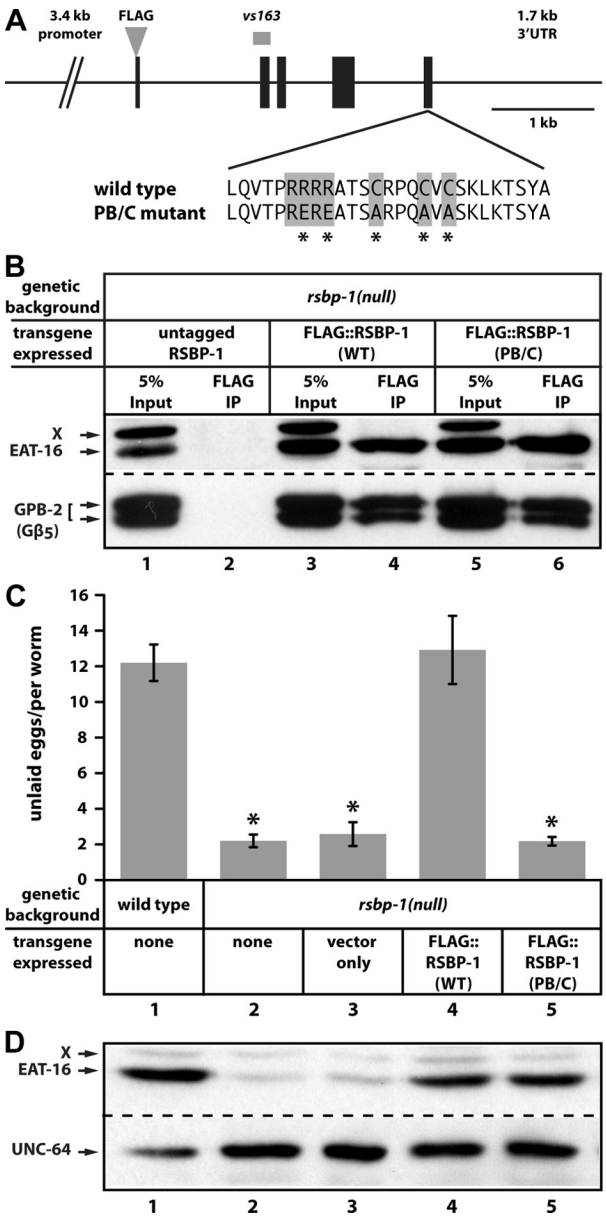

Figure 7. EAT-16 immunoprecipitation, function, and protein levels in animals expressing membrane-targeting deficient RSBP-1. (A) Schematic of the *rsbp-1* gene showing mutations made in the C-terminal membrane-targeting domain. Two of four arginines were changed to glutamate to neutralize the polybasic region, and three cysteines were changed to alanines to prevent palmitoylation. We refer to this as the PB/C mutant. (B) Anti-FLAG coimmunoprecipitation of the EAT-16·GBP-2/Gβ_5 complex from lysates of the indicated genotypes. Untagged RSBP-1 expressed in *rsbp-1(null)* mutants served as a negative control. Samples representing 5% of the input material (5% input) and the whole immunoprecipitated pellet (FLAG IP) were analyzed by Western blotting. Like wild-type FLAG::RSBP-1, membrane-targeting deficient FLAG::RSBP-1(PB/C) coimmunoprecipitated EAT-16 and GBP-2/Gβ_5, showing that the mutant protein can still interact with this complex. (C) Egg-laying behavior in the indicated genotypes. FLAG::RSBP-1(PB/C) does not rescue the hyperactive egg-laying defect of *rsbp-1(null)* mutants, showing it is not functional. Asterisks indicate values different from the wild-type control, with $p < 0.0001$. (D) EAT-16 protein levels in the indicated genotypes, determined by Western blotting. UNC-64/syntaxin is used as a loading control. Samples in lanes 1–5 correspond to the genotypes analyzed in bars 1–5 of C. FLAG::RSBP-1(PB/C) restores EAT-16 protein levels in *rsbp-1(null)* mutants.

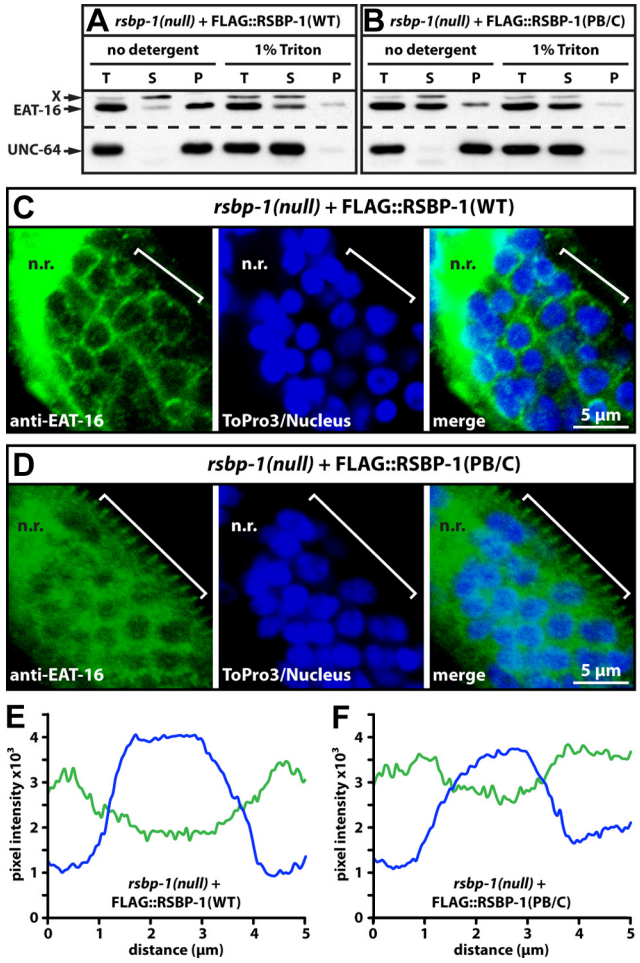

Figure 8. Subcellular localization of EAT-16 in animals expressing wild-type and targeting-deficient FLAG::RSBP-1. (A and B) Whole worm lysates of the indicated genotypes were fractionated with or without detergent, and total (T), supernatant/soluble (S), and pellet/membrane (P) fractions were analyzed by Western blotting. Anti-UNC-64/Syntaxin was used as a control membrane protein. In animals expressing wild-type FLAG::RSBP-1, EAT-16 is predominantly membrane-associated, whereas in animals expressing FLAG::RSBP- (PB/C) EAT-16 is predominantly soluble. (C and D) Representative immunostained images of clusters of neuronal cell bodies (brackets) in the *C. elegans* head, adjacent to the nerve ring (n.r.). Panels from left to right show, EAT-16 staining, nuclear staining with ToPro3, and a merged image. (E and F) Quantitative analysis of mean EAT-16 (green) and nuclear (blue) stain intensity across cells. In animals expressing wild-type FLAG::RSBP-1, EAT-16 staining was seen in tight rings around neuronal cell bodies and was separated from the nucleus by a thin ring of unstained cytoplasm, indicative of plasma membrane localization. However in animals expressing FLAG::RSBP- (PB/C) there is no separation of the nuclear from the EAT-16 stains suggesting cytosolic localization.

the putative membrane-targeting sequence of RSBP-1 is required for the membrane association of the EAT-16 complex.

Antibody staining confirmed that the RSBP-1 targeting sequence was required to localize endogenous EAT-16 to the plasma membrane of *C. elegans* neurons. In *rsbp-1(null)* animals expressing wild-type FLAG::RSBP-1 we observed EAT-16 staining in tight rings around neuronal cell bodies, indicative of plasma membrane localization (Figure 8C), as we had seen previously in wild-type animals (Supplemental Figure 2A). We further analyzed this localization by com-

paring the intensity of EAT-16 and nuclear staining across single cells. Although *C. elegans* neurons are very small with relatively large nuclei, we found a distinct separation of the apparently plasma membrane localized EAT-16 from the nucleus by a thin ring of unstained cytoplasm (Figure 8E). In contrast, EAT-16 staining was more diffuse in the neuronal cell bodies of animals expressing targeting-deficient FLAG::RSBP-1(PB/C), and the EAT-16 stain was no longer separated from the nuclear stain (Figure 8, D and F), suggesting EAT-16 was localized to the cytoplasm of these cells. Our results show that the membrane-targeting sequence of RSBP-1 is required to localize EAT-16 to the plasma membrane.

Combined with our evidence that the targeting sequence of RSBP-1 is absolutely required for EAT-16 function, we conclude that a primary function of RSBP-1 is to target EAT-16 to the plasma membrane and that plasma membrane localization is essential for EAT-16 to act as a regulator of $G\alpha_q$ signaling in *C. elegans* neurons.

DISCUSSION

R7 RGS Proteins Differ in Their Functional Requirement for Membrane Targeting

We have demonstrated that the EAT-16 complex requires membrane targeting by its RSBP-1 subunit to function as an inhibitor of $G\alpha_q$ signaling, whereas the EGL-10 complex does not associate with RSBP-1 and does not require RSBP-1 for its function as an inhibitor of $G\alpha_o$ signaling. All members of the R7 RGS family are highly similar; however, sequence analysis shows EGL-10 is most similar to mammalian RGS6 and RGS7, whereas EAT-16 is most similar to RGS9 and RGS11 (Sierra *et al.*, 2002; Porter and Koelle, 2009). Combined with our data and previous studies of the mammalian proteins this may indicate the existence of two evolutionarily conserved R7 RGS subfamilies with functional differences. We propose splitting the R7 RGS protein family into an RGS6/7 subfamily, of which EGL-10 would be a member, and an RGS9/11 subfamily, of which EAT-16 would be a member.

Members of the RGS9/11 subfamily appear to require membrane-targeting subunits for membrane association and function. Our data clearly show that EAT-16 depends on RSBP-1 for membrane association. Similarly, the subcellular targeting of mammalian RGS9-1·$G\beta_5$ in the rod outer segments requires the interaction of R9AP with the DEP domain of RGS9-1 (Martemyanov *et al.*, 2003), and membrane localization of neuronal RGS9-2·$G\beta_5$ requires R7BP (Anderson *et al.*, 2007a). RGS proteins act as GAPs toward $G\alpha$ subunits that are localized to the plasma membrane, and thus it has long been assumed that RGS proteins must also be targeted to the plasma membrane to carry out their functions as inhibitors of G protein signaling. Indeed, GAP activity of retinal RGS9-1 toward $G\alpha_t$ is strongly potentiated by membrane association via R9AP (Lishko *et al.*, 2002; Hu *et al.*, 2003). Thus our data showing EAT-16 requires membrane targeting by RSBP-1 for all detectable functions in vivo is consistent with these in vivo functions resulting from GAP activity toward $G\alpha_q$ and suggests that all members of the RGS9/11 subfamily require membrane localization by a targeting subunit to function as GAPs for their target G proteins.

EGL-10 is a member of the RGS6/7 subfamily, and we found no evidence that EGL-10 requires RSBP-1 for subcellular targeting or function. In addition we found that EGL-10 is a predominantly soluble protein. Similarly, studies in mammalian tissue showed that RGS7 in the retinal ON-bipolar cells is still correctly targeted in the absence of R7BP (Cao *et al.*, 2008) and found soluble pools of RGS7 in neurons (Cao *et al.*, 2008; Grabowska *et al.*, 2008). Thus members of the RGS6/7 subfamily do not appear to require a membrane-targeting subunit for function, although membrane association by other mechanisms is likely required for at lease some of the functions of this subfamily.

It has been proposed that R7 RGS complexes can migrate to intracellular sites and perform active signaling functions. Not only are members of the RGS6/7 subfamily found in soluble pools, but members of the RGS9/11 subfamily might also be released from the membrane under some circumstances because their membrane attachment depends on palmitoylation of their membrane-targeting subunit, and palmitoylation is a reversible modification. Indeed, artificially blocking palmitoylation causes R7 proteins to accumulate intracellularly in cultured cells (Drenan *et al.*, 2005, 2006). However, our results did not detect any intracellular localization or function of endogenous EAT-16 complexes. Antibody stains do not detect endogenous EAT-16 protein intracellularly, but rather show that it is restricted to the plasma membrane, and mutating the membrane-targeting sequence of RSBP-1 resulted in complete loss of EAT-16 function. If depalmitoylated, intracellular EAT-16 complexes had a positive function, we would instead have expected to observe a gain-of-function effect when we transgenically expressed the membrane-targeting mutant of RSBP-1. Although we cannot exclude the possibility that a small pool of EAT-16 complexes is depalmitoylated and carries out an active intracellular function, our experiments did not support this hypothesis. Thus we conclude that EAT-16 functions primarily at the plasma membrane to inhibit $G\alpha_q$ signaling. It remains to be determined whether members of the RGS6/7 subfamily play intracellular roles in regulating G protein signaling.

Differing Plasma Membrane–targeting Mechanisms May Determine Gα Specificity of R7 RGS Subfamilies

A small proportion of EGL-10 is found in the membrane fraction and this may be the active pool, but how this pool of EGL-10 is targeted to the membrane is not clear because its membrane association does not depend on RSBP-1. In addition to RSBP-1, other more divergent R7 RGS membrane-targeting subunits may exist. However, none have been found by either bioinformatic or pull down approaches in any organism to date, and two alternative mechanisms for R7 RGS membrane association have been suggested. First, it has been reported that RGS7 is palmitoylated and that its palmitoylation and subsequent membrane targeting are promoted by $G\alpha_o$ signaling (Rose *et al.*, 2000; Takida *et al.*, 2005). However, comparing RGS7 with EGL-10, we did not identify any conserved potential palmitoylation sites in these proteins. The second proposed mechanism is via direct interaction with a GPCR. Analysis of the Sst2 protein in yeast, which is distantly related to R7 RGS proteins and believed to be functionally analogous, found a direct interaction between the DEP domain of Sst2 and the GPCR, Ste2. This interaction brings Sst2 in close proximity to its target G protein, allowing it to exhibit efficient GAP activity (Ballon *et al.*, 2006). Subsequently Sandiford and coworkers showed that RGS7·$G\beta_5$ could directly interact with the third intracellular loop of muscarinic M3 receptors and inhibit $G\alpha_q$ signaling via a non-GAP mechanism (Sandiford and Slepak, 2009). Thus direct interaction with receptors that couple to a specific $G\alpha$ protein could direct EGL-10 and other RGS6/7 subfamily members toward their particular $G\alpha$ targets.

Similarly we propose that members of the RGS9/11 subfamily might be directed toward specific Gα targets by their membrane-binding subunits. In vitro experiments show that all mammalian R7 RGS·Gβ_5 complexes exhibit GAP activity specifically toward G$\alpha_{o/i}$ subunits (Hooks *et al.*, 2003). It has therefore remained a puzzle as to why genetic experiments in *C. elegans* have found that in vivo, whereas EGL-10 does specifically inhibit Gα_o, EAT-16 rather appears to specifically inhibit Gα_q (Koelle and Horvitz, 1996; Hajdu-Cronin *et al.*, 1999). The in vitro assays for Gα specificity of R7 RGS proteins were performed in the absence of a membrane binding subunit (Hooks *et al.*, 2003). Thus it is possible that in vitro results obtained for the membrane-targeting subunit independent RGS6/7 subfamily accurately represent the in vivo specificity of these proteins, but that the absence of the membrane-targeting subunits essential for function of the RGS9/11 subfamily prevented the in vitro assays of these proteins from showing proper Gα protein specificity. It would be interesting to determine whether the in vitro Gα specificity of the RGS9/11 subfamily could indeed be altered toward Gα_q by the inclusion of R7BP.

The hypothesis that membrane-targeting subunits could determine Gα specificity is consistent with previous work from our lab that used domain swapping experiments to show that the DEP/DHEX region of EGL-10 and EAT-16 determines specificity toward Gα_o versus Gα_q in vivo (Patikoglou and Koelle, 2002). Because the DEP/DHEX region has been show to interact with R9AP and R7BP (Baker *et al.*, 2006; Anderson *et al.*, 2007b), it is likely that this region also determines whether EGL-10 and EAT-16 associate with RSBP-1. Thus the domain swapping experiments support the hypothesis that RSBP-1 and its mammalian ortholog, R7BP, may direct RGS9/11 subfamily complexes to target Gα_q in vivo. We note that RGS9-1 in mammalian retina does not act on Gα_q, but rather on the G$\alpha_{i/o}$ family G protein, transducin. However, membrane anchoring of RGS9-1 in this specialized case is carried out not by R7BP, but rather by the transmembrane domain containing, divergent membrane-targeting subunit, R9AP, which may lack the Gα_q-specifying function we hypothesize for R7BP.

ACKNOWLEDGMENTS

We gratefully acknowledge Andreas Wissmann at NemaRx Pharmaceuticals (Calgary, Canada) for collecting the automated tracking data we analyzed in Figure 2. We thank Mike Nonet (Washington University) for the UNC-64 antibody, the National Bioresource Project of Japan for the *eat-16(tm761)* strain, and the confocal facilities of the Yale Center for cell and molecular imaging. This work was funded by National Institutes of Health Grants NS36918 and MH082201.

REFERENCES

Anderson, G., Lujan, R., Semenov, A., Pravetoni, M., Posokhova, E., Song, J., Uversky, V., Chen, C., Wickman, K., and Martemyanov, K. (2007a). Expression and localization of RGS9-2·Gβ_5·R7BP complex *in vivo* is set by dynamic control of its constitutive degradation by cellular cysteine proteases. J. Neurosci. *27*, 14117–14127.

Anderson, G., Semenov, A., Song, J., and Martemyanov, K. (2007b). The membrane anchor R7BP controls the proteolytic stability of the striatal specific RGS protein, RGS9-2. J. Biol. Chem. *282*, 4772–4781.

Anderson, G., Posokhova, E., and Martemyanov, K. (2009). The R7 RGS protein family: multi-subunit regulators of neuronal G protein signaling. Cell. Biochem. Biophys. *54*, 33–46.

Baker, S., Martemyanov, K., Shavkunov, A., and Arshavsky, V. (2006). Kinetic mechanism of RGS9-1 potentiation by R9AP. Biochemistry *45*, 10690–10697.

Ballon, D., Flanary, P., Gladue, D., Konopka, J., Dohlman, H., and Thorner, J. (2006). DEP-domain-mediated regulation of GPCR signaling responses. Cell *126*, 1079–1093.

Bastiani, C., and Mendel, J. (2006). Heterotrimeric G proteins in *C. elegans* (October 2006), WormBook, The *C. elegans* Research Community, doi/10.1895/wormbook. 1.75.1, http://www.wormbook.org.

Brenner, S. (1974). The genetics of *Caenorhabditis elegans*. Genetics *77*, 71–94.

Brundage, L., Avery, L., Katz, A., Kim, U., Mendel, J., Sternberg, P., and Simon, M. (1996). Mutations in a *C. elegans* Gα_q gene disrupt movement, egg laying, and viability. Neuron *16*, 999–1009.

Bryson, K., McGuffin, L., Marsden, R., Ward, J., Sodhi, J., and Jones, D. (2005). Protein structure prediction servers at University College London. Nucleic Acids Res. *33*, W36–38.

Cao, Y., Song, H., Okawa, H., Sampath, A., Sokolov, M., and Martemyanov, K. (2008). Targeting of RGS7·Gβ_5 to the dendritic tips of ON-bipolar cells is independent of its association with membrane anchor R7BP. J. Neurosci. *28*, 10443–10449.

Chase, D., Patikoglou, G., and Koelle, M. (2001). Two RGS proteins that inhibit Gα_o and Gα_q signaling in *C. elegans* neurons require a Gβ_5-like subunit for function. Curr. Biol. *11*, 222–231.

Chase, D., and Koelle, M. (2004). Genetic analysis of RGS protein function in *Caenorhabditis elegans*. Methods Enzymol. *389*, 305–320.

Cheever, M., Snyder, J., Gershburg, S., Siderovski, D., Harden, T., and Sondek, J. (2008). Crystal structure of the multifunctional Gβ_5·RGS9 complex. Nat. Struct. Mol. Biol. *15*, 155–162.

Chen, C., Burns, M., He, W., Wensel, T., Baylor, D., and Simon, M. (2000). Slowed recovery of rod photoresponse in mice lacking the GTPase accelerating protein RGS9-1. Nature *403*, 557–560.

Drenan, R., Doupnik, C., Boyle, M., Muglia, L., Huettner, J., Linder, M., and Blumer, K. (2005). Palmitoylation regulates plasma membrane-nuclear shuttling of R7BP, a novel membrane anchor for the RGS7 family. J. Cell Biol. *169*, 623–633.

Drenan, R., Doupnik, C., Jayaraman, M., Buchwalter, A., Kaltenbronn, K., Huettner, J., Linder, M., and Blumer, K. (2006). R7BP augments the function of RGS7·Gβ_5 complexes by a plasma membrane-targeting mechanism. J. Biol. Chem. *281*, 28222–28231.

Finney, M., and Ruvkun, G. (1990). The *unc-86* gene product couples cell lineage and cell identity in *C. elegans*. Cell *63*, 895–905.

Gish, W. (1996–2006). BLASTP 2.0MP-WashU algorithm. http://blast.wustl.edu/.

Grabowska, D., Jayaraman, M., Kaltenbronn, K., Sandiford, S., Wang, Q., Jenkins, S., Slepak, V., Smith, Y., and Blumer, K. (2008). Postnatal induction and localization of R7BP, a membrane-anchoring protein for regulator of G protein signaling 7 family-Gβ_5 complexes in brain. Neuroscience *151*, 969–982.

Hajdu-Cronin, Y., Chen, W., Patikoglou, G., Koelle, M., and Sternberg, P. (1999). Antagonism between Gα_o and Gα_q in *Caenorhabditis elegans*: the RGS protein EAT-16 is necessary for Gα_o signaling and regulates Gα_q activity. Genes Dev. *13*, 1780–1793.

Hamm, H. (1998). The many faces of G protein signaling. J. Biol. Chem. *273*, 669–672.

Hess, H.A., Reinke, V., and Koelle, M.R. (2006). Construction and screening of deletion mutant libraries to generate *C. elegans* gene knockouts. In: Reverse Genetics (April 2006), ed. J. Ahringer, WormBook, The *C. elegans* Research Community, doi/10.1895/wormbook. 1.47.1, http://www.wormbook.org.

Hooks, S., Waldo, G., Corbitt, J., Bodor, E., Krumins, A., and Harden, T. (2003). RGS6, RGS7, RGS9, and RGS11 stimulate GTPase activity of Gα_i family G-proteins with differential selectivity and maximal activity. J. Biol. Chem. *278*, 10087–10093.

Hu, G., and Wensel, T. (2002). R9AP, a membrane anchor for the photoreceptor GTPase accelerating protein, RGS9-1. Proc. Natl. Acad. Sci. USA *99*, 9755–9760.

Hu, G., Zhang, Z., and Wensel, T. (2003). Activation of RGS9-1 GTPase acceleration by its membrane anchor, R9AP. J. Biol. Chem. *278*, 14550–14554.

Jayaraman, M., Zhou, H., Jia, L., Cain, M., and Blumer, K. (2009). R9AP and R7BP: traffic cops for the RGS7 family in phototransduction and neuronal GPCR signaling. Trends Pharmacol. Sci. *30*, 17–24.

Jones, D. (1999). Protein secondary structure prediction based on position-specific scoring matrices. J. Mol. Biol. *292*, 195–202.

Keresztes, G., Mutai, H., Hibino, H., Hudspeth, A., and Heller, S. (2003). Expression patterns of the RGS9-1 anchoring protein R9AP in the chicken and mouse suggest multiple roles in the nervous system. Mol. Cell. Neurosci. *24*, 687–695.

Keresztes, G., Martemyanov, K., Krispel, C., Mutai, H., Yoo, P., Maison, S., Burns, M., Arshavsky, V., and Heller, S. (2004). Absence of the RGS9·Gβ_5

GTPase-activating complex in photoreceptors of the R9AP knockout mouse. J. Biol. Chem. *279*, 1581–1584.

Koelle, M., and Horvitz, H. (1996). EGL-10 regulates G protein signaling in the *C. elegans* nervous system and shares a conserved domain with many mammalian proteins. Cell *84*, 115–125.

Laemmli, U. (1970). Cleavage of structural proteins during the assembly of the head of bacteriophage T4. Nature *227*, 680–685.

Lishko, P., Martemyanov, K., Hopp, J., and Arshavsky, V. (2002). Specific binding of RGS9·$G\beta_{5L}$ to protein anchor in photoreceptor membranes greatly enhances its catalytic activity. J. Biol. Chem. *277*, 24376–24381.

Martemyanov, K., *et al.* (2003). The DEP domain determines subcellular targeting of the GTPase activating protein RGS9 *in vivo.* J. Neurosci. *23*, 10175–10181.

Martemyanov, K., Yoo, P., Skiba, N., and Arshavsky, V. (2005). R7BP, a novel neuronal protein interacting with RGS proteins of the R7 family. J. Biol. Chem. *280*, 5133–5136.

Mello, C., and Fire, A. (1995). DNA transformation. Methods Cell Biol. *48*, 451–482.

Mendel, J., Korswagen, H., Liu, K., Hajdu-Cronin, Y., Simon, M., Plasterk, R., and Sternberg, P. (1995). Participation of the protein $G\alpha_o$ in multiple aspects of behavior in *C. elegans*. Science *267*, 1652–1655.

Nishiguchi, K., Sandberg, M., Kooijman, A., Martemyanov, K., Pott, J., Hagstrom, S., Arshavsky, V., Berson, E., and Dryja, T. (2004). Defects in RGS9 or its anchor protein R9AP in patients with slow photoreceptor deactivation. Nature *427*, 75–78.

Patikoglou, G., and Koelle, M. (2002). An N-terminal region of *Caenorhabditis elegans* RGS proteins EGL-10 and EAT-16 directs inhibition of $G\alpha_o$ versus $G\alpha_q$ signaling. J. Biol. Chem. *277*, 47004–47013.

Popov, S., Yu, K., Kozasa, T., and Wilkie, T. (1997). The regulators of G protein signaling (RGS) domains of RGS4, RGS10, and GAIP retain GTPase activating protein activity *in vitro.* Proc. Natl. Acad. Sci. USA *94*, 7216–7220.

Porter, M., and Koelle, M. (2009). Insights into RGS protein function from studies in *Caenorhabditis elegans*. Progress Mol. Biol. Trans. Sci. *86*, 15–47.

Robatzek, M., Niacaris, T., Steger, K., Avery, L., and Thomas, J. (2001). eat-11 encodes GPB-2, a $G\beta_5$ ortholog that interacts with $G\alpha_o$ and $G\alpha_q$ to regulate *C. elegans* behavior. Curr. Biol. *11*, 288–293.

Rose, J., Taylor, J., Shi, J., Cockett, M., Jones, P., and Hepler, J. (2000). RGS7 is palmitoylated and exists as biochemically distinct forms. J. Neurochem. *75*, 2103–2112.

Ross, E., and Wilkie, T. (2000). GTPase-activating proteins for heterotrimeric G proteins: regulators of G protein signaling (RGS) and RGS-like proteins. Annu. Rev. Biochem. *69*, 795–827.

Rost, B., Yachdav, G., and Liu, J. (2004). The PredictProtein server. Nucleic Acids Res. *32*, W321–W326.

Sandiford, S., and Slepak, V. (2009). $G\beta_5$·RGS7 selectively inhibits muscarinic M3 receptor signaling via the interaction between the third intracellular loop of the receptor and the DEP domain of RGS7. Biochemistry *48*, 2282–2289.

Schafer, W. (2005). Egg-laying (December 2005), WormBook, The *C. elegans* Research Community, doi/10.1895/wormbook. 1.38.1, http://www.wormbook.org.

Sierra, D., *et al.* (2002). Evolution of the regulators of G-protein signaling multigene family in mouse and human. Genomics *79*, 177–185.

Snow, B., Krumins, A., Brothers, G., Lee, S., Wall, M., Chung, S., Mangion, J., Arya, S., Gilman, A., and Siderovski, D. (1998). A G protein γ subunit-like domain shared between RGS11 and other RGS proteins specifies binding to $G\beta_5$ subunits. Proc. Natl. Acad. Sci. USA *95*, 13307–13312.

Song, J., Waataja, J., and Martemyanov, K. (2006). Subcellular targeting of RGS9-2 is controlled by multiple molecular determinants on its membrane anchor, R7BP. J. Biol. Chem. *281*, 15361–15369.

Song, J., Song, H., Wensel, T., Sokolov, M., and Martemyanov, K. (2007). Localization and differential interaction of R7 RGS proteins with their membrane anchors R7BP and R9AP in neurons of vertebrate retina. Mol. Cell. Neurosci. *35*, 311–319.

Subramaniam, S. (1998). The Biology Workbench—a seamless database and analysis environment for the biologist. Proteins *32*, 1–2.

Ségalat, L., Elkes, D., and Kaplan, J. (1995). Modulation of serotonin-controlled behaviors by $G\alpha_o$ in *Caenorhabditis elegans*. Science *267*, 1648–1651.

Takida, S., Fischer, C., and Wedegaertner, P. (2005). Palmitoylation and plasma membrane targeting of RGS7 are promoted by $G\alpha_o$. Mol. Pharmacol. *67*, 132–139.

van der Linden, A., Simmer, F., Cuppen, E., and Plasterk, R. (2001). The G-protein β-subunit GPB-2 in *Caenorhabditis elegans* regulates the $G\alpha_o$-$G\alpha_q$ signaling network through interactions with the regulator of G-protein signaling proteins EGL-10 and EAT-16. Genetics *158*, 221–235.